

# Reaction Cross Sections and Rate Constants for the Cl + H<sub>2</sub> Reaction from Quasiclassical Trajectory Calculation on Two New ab Initio Potential Energy Surfaces

Changsheng Shen,<sup>†</sup> Tao Wu,<sup>†</sup> Guanzhi Ju,<sup>\*,†,‡</sup> and Wensheng Bian<sup>§</sup>

State Key Laboratory of Coordination Chemistry, Mesoscopic Solid State Chemistry Institute, Department of Chemistry, Nanjing University, Nanjing 210093, P. R. China, State Key Laboratory of Crystal Material, Shandong University, Jinan 250100, P. R. China, and Institute of Theoretical Chemistry, Shandong University, Jinan 250100, P.R. China

Received: June 26, 2001; In Final Form: October 17, 2001

The reaction cross sections and rate constants for the Cl + H<sub>2</sub> → HCl + H reaction have been calculated by quasiclassical trajectory (QCT) method with symplectic integral on two new three-dimensional ab initio potential energy surfaces (PES), BW2 and mBW2. The reaction cross sections of these reactions increase with the H<sub>2</sub> rotational quantum number *j* at a given collision energy and vibrational quantum number *v* = 0. The effectivity of rotational energy on the reaction is compared with that of translational energy.

## I. Introduction

The Cl + H<sub>2</sub> reaction, just as the H + H<sub>2</sub> and F + H<sub>2</sub> reactions, has been concerned for nearly a century by theoretical and experiential chemists.<sup>1–14</sup> Kumaran and co-workers<sup>15</sup> have summarized the extensive experimental work on rate constants for the Cl + H<sub>2</sub> reaction and its isotopic variants. Persky and co-workers<sup>16–20</sup> performed quasiclassical trajectory calculations (QCT) for the Cl + H<sub>2</sub> reaction and isotopic variants on a semiempirical LEPS (London–Eyring–Polanyi–Sato) PES, originally called GSW. The energy dependence of the reaction cross section, thermal rate constants, and the product energy partitioning were calculated for all the isotopomers of H<sub>2</sub>.<sup>17–20</sup> In particular, reaction cross section (*S<sub>r</sub>*), thermal rate constants (*k<sub>T</sub>*) isotopic branching ratios, and the product energy partitioning for the Cl + H<sub>2</sub>,<sup>17</sup> Cl + D<sub>2</sub>,<sup>18</sup> and Cl + HD<sup>19</sup> reactions were calculated over a wide range of collision energies, *E<sub>c</sub>*, and initial H<sub>2</sub> (D<sub>2</sub>, HD) vibrational state *v* = 0 and rotational states *j* = 0–4(5,4). Aoiz and Bañares<sup>21</sup> performed QCT calculation for the Cl + H<sub>2</sub> (D<sub>2</sub>) reactions on partly ab initio the PES, called the G3 PES.<sup>10</sup> They calculated cross sections (*S<sub>r</sub>*), thermal rate constants (*k<sub>T</sub>*), and the kinetic isotopic effect (KIE) over a wide range of collision energies, *E<sub>c</sub>*, and initial H<sub>2</sub>(D<sub>2</sub>) vibrational state *v* = 0 and rotational states *j* = 0–5(6).

Although the G3 PES is a significant improvement over previous potential surfaces, the HCl + D/DCI + H branching ratios presented by the recent molecular beam experiment<sup>12</sup> for Cl + HD at low collision energies are in strong disagreement with QM calculations on the G3 potential surface. To further improve the PES for the Cl + H<sub>2</sub> reaction, a new ab initio PES called BW2 was constructed by Bian and Werner.<sup>22</sup> On the BW2 PES, Manthe<sup>23</sup> and Yang<sup>24,25</sup> carried out quantum dynamics studies of Cl + H<sub>2</sub> reaction and Cl + D<sub>2</sub> reaction. They compared calculated results with experimental results.

However, the BW2 PES does not include the spin–orbit (SO) effect, while the previous PESs, such as the GQQ and G3 PES,

include the SO effect. Therefore, a modified version of the BW2 PES called mBW2,<sup>26</sup> which includes spin–orbit coupling approximately, is constructed using similar scaling way as G3 and GQQ PES. In this work, we report the results of a quasiclassical trajectory calculation on BW2 and mBW2 PESs. To test the new full ab initio PESs, *S<sub>r</sub>* and *k<sub>T</sub>* are also calculated over a wide range of collision energies, *E<sub>c</sub>*, and initial H<sub>2</sub> vibrational state *v* = 0 and rotational states *j* = 0–4. The results are discussed and compared with calculations on other surfaces and experimental measurements.

The organization of this paper is as follows: section II introduces the BW2 and mBW2 PESs. Computational details are briefly presented in section III. The results of the calculation and a discussion of the results are given in section IV. Finally, a summary is presented in section V.

## II. Potential Energy Surface

The BW1 PES<sup>22</sup> was computed using internally contracted multireference configuration interaction (MRCI) wave functions<sup>27</sup> with complete active-space self-consistent field (CASSCF) reference wave functions.<sup>28</sup> The Davidson correction<sup>29</sup> (+Q) was applied to the final energies in order to account approximately for unlinked cluster effects of higher excitations. The analytical fits were generated from the computed energies at 1200 geometries. The BW1 is based on the original MRCI + Q energies without scaling; the BW2 was generated from the scaled energies, similar to what was done in Truhler's scaled external correlation (SEC) correction,<sup>30</sup> i.e.

$$E_{\text{Scaled}} = F(E_{\text{MRCI+Q}} - E_{\text{CASSCF}}) + E_{\text{CASSCF}} \quad (1)$$

The scaling factor *F* is 1.05485 in BW2 surface, excluding the spin–orbit effect.

The mBW2 PES, used in our QCT calculations, is a modified version of BW2, which includes spin–orbit coupling approximately. The *F* can be determined so that the dissociation energies of the diatomic molecules are reproduced correctly:

$$F = \frac{D_e(\text{exp}) - D_e(\text{CASSCF})}{D_e(\text{MRCI} + \text{Q}) - D_e(\text{CASSCF})} \quad (2)$$

\* Corresponding author. E-mail: gzju@nju.edu.cn.

<sup>†</sup> State Key Laboratory of Coordination Chemistry, Nanjing University.

<sup>‡</sup> State Key Laboratory of Crystal Material, Shandong University.

<sup>§</sup> Institute of Theoretical Chemistry, Shandong University.

**TABLE 1: Comparison of Barrier Properties for the Cl + H<sub>2</sub> Reaction**

surface	$R_{\text{ClH}}^a$	$R_{\text{HH}}^a$	$\Theta^b$	$E^c$	$\omega_i^d$	$\omega_b^e$	$\omega_s^f$
G3	2.648	1.870	180	7.88	1520i	581	1358
BW1	2.710	1.850	180	8.14	1333i	543	1356
BW2	2.704	1.854	180	7.61	1294i	540	1360
mBW2	2.708	1.850	180	7.88	1317i	542	1358

<sup>a</sup> Bond distance in bohr. <sup>b</sup> Bond angle in deg. <sup>c</sup> Barrier height in kcal/mol. <sup>d</sup> Imaginary frequency in cm<sup>-1</sup>. <sup>e</sup> Bending vibration frequency in cm<sup>-1</sup>. <sup>f</sup> Symmetric stretching vibration frequency in cm<sup>-1</sup>.

where  $D_e$ 's are the calculated and experimental dissociation energies of HCl or H<sub>2</sub>. The experimental dissociation energy of HCl has been corrected for the spin-orbit effect.

The analytic form of the BW surfaces (BW1, BW2, mBW2) is given by

$$V_{\text{ABC}} = \sum_i V_i^{(1)} + \sum_n V_n^{(2)}(R_n) + V_{\text{ABC}}^{(3)}(R_{\text{AB}}, R_{\text{BC}}, R_{\text{AC}}) \quad (3)$$

where  $V_i^{(1)}$ 's ( $i = A, B, C$ ) are the energies of the atoms,  $V_n^{(2)}$ 's ( $n = \text{AB}, \text{BC}, \text{AC}$ ) are the diatomic potentials of HCl and H<sub>2</sub>, and  $V_{\text{ABC}}^{(3)}$ 's is a three-body potential. The diatomic potentials are expressed as

$$V_{\text{AB}} = \frac{C_0 e^{(-\alpha_{\text{AB}} R_{\text{AB}})}}{R_{\text{AB}}} + \sum_{i=1}^6 c_i \rho_{\text{AB}}^i \quad (4)$$

with

$$\rho_{\text{AB}} = R_{\text{AB}} e^{(-\beta_{\text{AB}} R_{\text{AB}})} \quad (5)$$

The three-body potential is expressed as a polynomial of order  $M$

$$V_{\text{ABC}}^{(3)}(R_{\text{AB}}, R_{\text{BC}}, R_{\text{AC}}) = \sum_{i,j,k}^M d_{ijk} \rho_{\text{AB}}^i \rho_{\text{BC}}^j \rho_{\text{AC}}^k \quad (6)$$

with the constraints  $i + j + k \neq i \neq j \neq k$  and  $M \geq i + j + k$ . For the sake of symmetry, we have set  $d_{ijk} = d_{kji}$  and  $\beta_{\text{AB}} = \beta_{\text{AC}}$ . The three-body parameters were determined by fitting the difference of the ab initio energies of the ClH<sub>2</sub> system and the sum of the one- and two-body energies at the corresponding geometries.

All of the parameters of mBW2 surface can be downloaded from the web.<sup>26</sup>

The BW surfaces (BW1, BW2, mBW2) differ qualitatively from G3 surface in the entrance and exit channels. The BW surfaces have long-range van der Waals minima, which are entirely absent in the LEPS-type G3 surface. In the entrance channel, the BW surfaces are least repulsive for perpendicular (T-shaped) approach of Cl to H<sub>2</sub>, while G3 surface is most repulsive for T-shaped structure. The BW surfaces have a well in the exit channel as in the entrance channel. The comparison of the saddle point properties of BW and G3 surfaces are presented in Table 1. It is found that the saddle points of the BW surfaces are located earlier in the entrance channel than that of the G3 surface. The barrier height of the mBW2 surface is equal to that of the G3 surface. However, the mBW2 imaginary frequency corresponding to the asymmetric stretch is substantially smaller than the G3 value, indicating that the G3 barrier is somewhat thinner.

### III. Computational Details

A homemade QCT procedure was used for trajectory calculation. The computational details have been described by Karplus,

**TABLE 2: Threshold Energies (in eV) for the Cl + H<sub>2</sub>( $v = 0, j = 0-4$ ) Reaction Calculated on Every PES**

$j$	BW2	mBW2	G3 <sup>21</sup>	GSW <sup>17</sup>
0	0.22	0.21	0.149	0.143
1	0.20	0.18	0.176	0.160
2	0.14	0.14	0.209	0.186
3	0.14	0.15	0.238	0.208
4	0.14	0.14	0.248	0.208

Porter, and Sharma.<sup>31</sup> In our previous work,<sup>32,33</sup> we found the Runge-Kutta method provided worse conservation of energy. To maintain the conservational property in numerical solution of Hamiltonian systems, we applied symplectic integral method<sup>34-36</sup> in QCT study. The step size used in all calculations reported here was  $1.08 \times 10^{-16}$ s.

### IV. Results and Discussion

**1. Reaction Cross Sections.** On BW2 and mBW2 PESs, calculations were carried out for the initial vibrational state  $v = 0$ , rotational states  $j = 0-4$ , and collision energies  $E_c$  (11-18 values of  $E_c$  for each  $j$  state) in the range between threshold and 0.8 eV. Batches of 10000 trajectories were run for every set of  $j$  and  $E_c$ .

The reaction cross sections  $S_r(v, j, E_c)$  for a set of initial conditions were calculated from the equation

$$S_r(v, j, E_c) = \pi b_{\text{max}}^2(E_c) [N_r(v, j, E_c) / N(v, j, E_c)] \quad (7)$$

where  $N_r(v, j, E_c)$  and  $N(v, j, E_c)$  are the number of reactive collisions and the number of total collisions, respectively. The  $b_{\text{max}}(E_c)$  is the maximum impact parameter.

Table 2 lists the calculated threshold energies as a function of the  $j$  state of the H<sub>2</sub> diatom. On the BW2 PES, the threshold value decreases with increasing  $j$  from 0 to 2; when  $j$  turns from 2 to 3 or 4, the threshold value does not change. On the mBW2 PES, the phenomenon is similar, except  $j = 3$ . However, on the G3 or GSW PES, the phenomenon is different, the threshold value increases with increasing  $j$ . When  $v = 0$  and  $j \leq 1$ , the threshold energy on BW2 and mBW2 PESs is higher than that on G3 and GSW PESs with the same  $j$ . However, when  $v = 0$  and  $j \geq 2$ , the threshold energy on BW2 and mBW2 PESs is lower than that on the G3 and GSW PES with the same  $j$ . It indicates that a T-shaped van der Waals well in entrance channel of the BW PES has an effect on the reaction. When  $j = 0$  or 1, the transformation from the T-shaped structure to collinear structure of the transition state is a little hard, so the threshold value on the BW PES is higher. When  $j$  increases, the transformation becomes easy, so the threshold value on the BW PES decreases, while on G3 and GSW PESs, the three atoms are collinear. The diatom rotation has a negative effect on reactivity, so the threshold value increases with  $j$ .

The reaction cross sections for the Cl + H<sub>2</sub> reaction calculated on BW2 and mBW2 PESs are shown in Figure 1. In most cases, the reaction cross section increases smoothly with different rate as collision energy increases. An increase of the H<sub>2</sub> rotational quantum number results in higher values of the cross sections at a given  $E_c$ .

Persky carried out QCT calculations for Cl + H<sub>2</sub> reaction on the GSW PES.<sup>17</sup> He found that at low collision energies the reaction cross sections decrease as  $j$  increases, while at high collision energies the reaction cross section is practically independent of  $j$ . The threshold values gradually increase with  $j$  until  $j = 4$ .

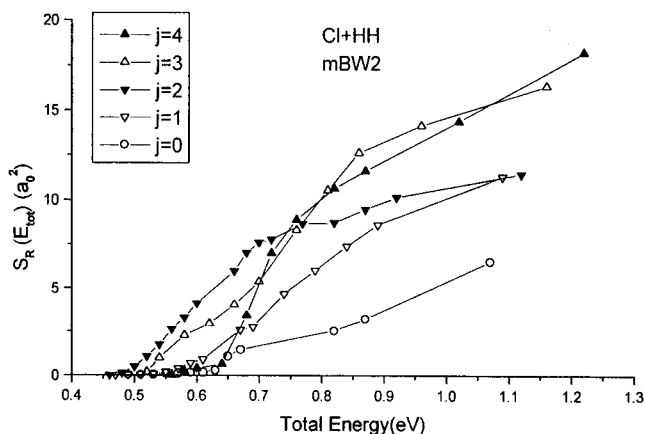
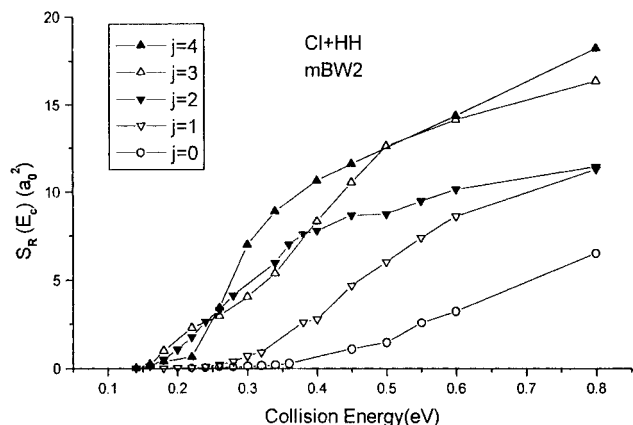
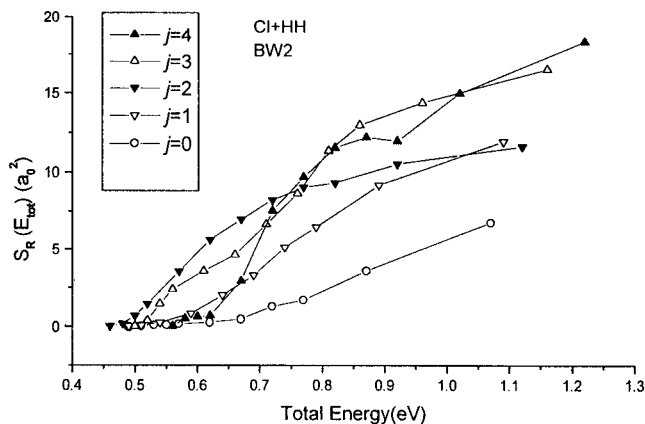
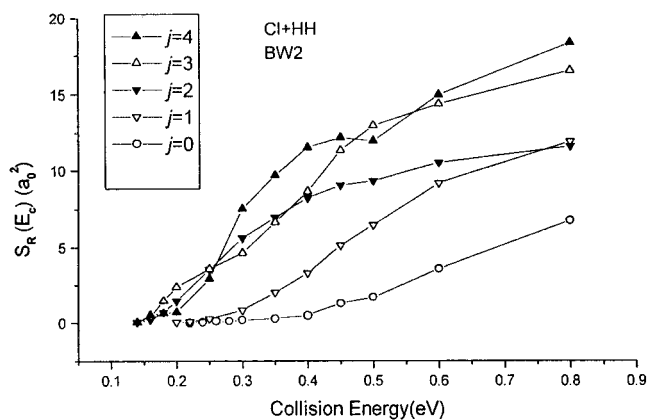


**Figure 1.** Reaction cross section as a function of collision energy calculated by QCT on BW2 and mBW2 PESs for the Cl + H<sub>2</sub> ( $v = 0$ ,  $j = 0-4$ ) reaction.

Aoiz and Bañares<sup>21</sup> performed QCT calculations for Cl + H<sub>2</sub> reaction on the G3 PES. He found the reaction cross section clearly decreases with  $j$ . The threshold values increase with  $j$  until  $j = 5$ .

The calculations on GSW and G3 PESs show a very similar behavior. These effects are characteristic of strongly collinear potential surfaces, but they are different from our work on BW2 and mBW2 PESs. However, the experiment<sup>11</sup> showed that the reaction cross section of  $j = 1$  was larger than that of  $j = 0$  in the same collision energy. Our calculation results on BW2 and mBW2 PESs accord with the experiment.<sup>11</sup> In addition, Yang<sup>24</sup> carried out quantum dynamic studies of Cl + H<sub>2</sub> reaction on the BW2 PES. He found that the reaction probability increases in general with increasing  $j$  at low collision energies. He also carried out quantum dynamic studies of Cl + D<sub>2</sub> reaction<sup>25</sup> on the BW2 PES. He pointed out that the reaction cross sections increase as  $j$  increases. We may believe that this is the important character of the BW PES. Moreover, for the F + H<sub>2</sub><sup>37</sup> and F + D<sub>2</sub><sup>38</sup> reactions on the SW PES,<sup>39</sup> the general trend is also that the cross sections increase with both the collision energy and the rotational quantum number of the H<sub>2</sub> or D<sub>2</sub> molecule.

To compare effectivity of rotational energy with that of translational energy, the dependence of  $S_r$  on total energy  $E_{\text{tot}}$  is displayed in Figure 2. For the Cl + H<sub>2</sub> reaction, at high total energies ( $E_{\text{tot}} > 0.75$  eV), the cross sections increase with increasing  $j$ . It shows that the rotational energy is more effective than translation energy when the total energy is the same, while at low total energies, the cross sections are the highest in  $j = 2$ .

**2. Rate Constants.** The reaction cross sections were used to calculate state-selected rate constants  $k(T, v=0, j)$  as a function

**Figure 2.** Reaction cross section as a function of total energy calculated by QCT on BW2 and mBW2 PESs for the Cl + H<sub>2</sub> ( $v = 0$ ,  $j = 0-4$ ) reaction.

of temperature for each of the initial  $j$ . The rate constant is given by the equation<sup>17</sup>

$$k(T, v=0, j) = (2/k_B T)^{3/2} (\pi \mu)^{-1/2} \int_0^\infty \sigma_r(v, j, E_c) E_c \exp(-E_c/k_B T) dE_c \quad (8)$$

where  $k_B$  is the Boltzmann constant and  $\mu$  is the reduced mass of the reaction system.

Calculated values of  $k(T, v=0, j)$  are displayed in Figure 3. As can be seen, all of lines are straight and in almost the same slope, which mean the activity energies are almost the same. Compared the results of the BW2 PES with those of the mBW2 PES, the trend of change is similar, except that the numerical values is a little different.  $k(T, v=0, j)$  increases with increasing  $j$  from  $j = 0$  to  $j = 3$ , and there is no significant difference between  $j = 2$  and  $j = 4$ .

Thermal rate constants  $k(T)$  were obtained between 200 and 450 K from the  $k(T, v=0, j)$  after the appropriate weighting  $p_{0,j}(T)$  with distribution of rotational states of the H<sub>2</sub> molecules including the H<sub>2</sub> nuclear spin weights<sup>21</sup>

$$k'(T) = \sum p_{0,j}(T) k(T, v=0, j) \quad (9)$$

To make the results directly comparable with the experiments, Tully<sup>40</sup> recommended dividing the rate constants obtained from trajectory by the factor  $[2 + \exp(-\Delta E/k_B T)]$ . The expression is

$$k(T) = k'(T) / [2 + \exp(-\Delta E/k_B T)] \quad (10)$$

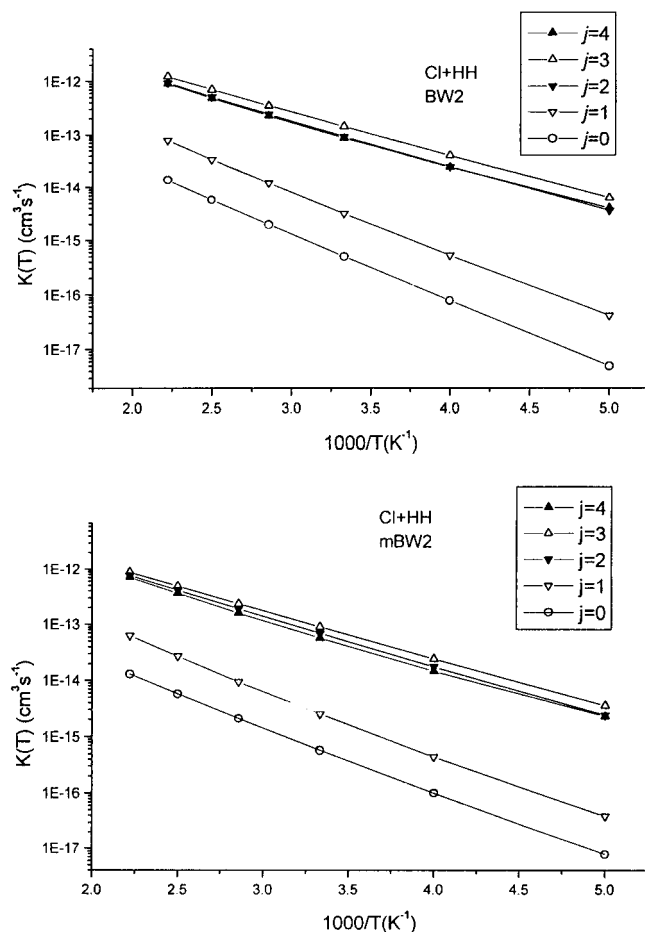


**Figure 3.** State-selected rate constants  $k(T, v=0, j=0-4)$  as a function of  $1000/T$  for the Cl + H<sub>2</sub> reaction.

where  $\Delta E$  is the energy fine-structure splitting between the two states,  $^2P_{3/2}$  and  $^2P_{1/2}$ , taken as  $10.6 \text{ kJ mol}^{-1}$ .

However, Manthe et al.<sup>23</sup> proposed that the BW2 surface does not include the spin-orbit (SO) interaction. Thus, the expression of rate constant is

$$k(T) = k'(T) \left\{ 2 \exp\left(\frac{1}{3} \frac{\Delta E}{kT}\right) + \exp\left(-\frac{2}{3} \frac{\Delta E}{kT}\right) \right\} \quad (11)$$

Rate constants  $k(T)$  on BW2 and mBW2 surfaces are shown in Figure 4. The experimental values<sup>15,41</sup> and the theoretical values on the BW2<sup>23</sup> PES from QM and on G3<sup>21</sup> and GSW<sup>17</sup> PESs from QCT are also plotted for comparison. For the Cl + H<sub>2</sub> reaction, the theoretical values on G3<sup>21</sup> and GSW<sup>17</sup> surfaces from QCT greatly agree with the experiment at higher temperatures, but the results are somewhat larger than those from the experiment at lower temperatures. In fact, this phenomenon is unreasonable because QCT calculations, which neglect the tunneling effects, should be somewhat smaller than the experiment. The rate constant modified by using eq 10 on BW2 surface and the QM result on the BW2 PES<sup>23</sup> are almost same. The results in general are in agreement with the experiment at higher temperatures, but the results are somewhat smaller than those of the experiment. However, the rate constants modified by using eq 11 on BW2 surface are much smaller than those of the experiment. The QCT results on the mBW2 PES are a little smaller than those of the experiment. However, they are a little larger than the rate constants modified by using eq 11 on BW2 surface. From this point, it can be seen that the inclusion of the

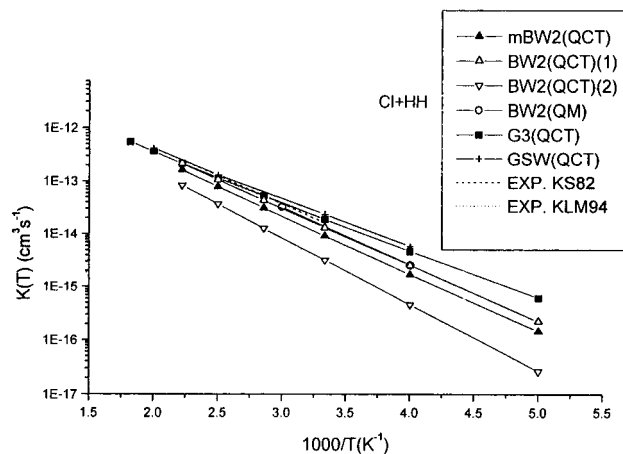


**Figure 4.** Comparison of thermal rate constants from experiment and theory for the Cl + H<sub>2</sub> reaction. mBW2(QCT) is the present QCT calculation on the mBW2 PES. BW2(QCT)(1) is the present calculation modified by using eq 10 on the BW2 surface; BW2(QCT)(2) is the present calculation modified by using eq 11 on the BW2 surface. BW2(QM) is the QM result on the BW2 PES.<sup>23</sup> G3(QCT) is the QCT result on the G3 PES.<sup>21</sup> GSW(QCT) is the QCT result<sup>17</sup> on the GSW PES. Exp is the experimental data.<sup>15,37</sup>

spin-orbit (SO) interaction and the difference of their transition state properties (see Table 1 and ref 26) make mBW2 better than BW2.

## V. Conclusion

In a summary, the following conclusions can be obtained for Cl + H<sub>2</sub> reaction on BW2 and mBW2 PESs by QCT calculations:

- (1) When  $v = 0$  and  $j \leq 1$ , the threshold energy on BW2 and mBW2 PESs is higher than that on G3 and GSW PESs with the same  $j$ . However, when  $v = 0$  and  $j \geq 2$ , the threshold energy on BW2 and mBW2 PESs is lower than that on G3 and GSW PESs with the same  $j$ .
- (2) The cross sections increase with the H<sub>2</sub> rotational quantum number  $j$  at a given  $E_c$  on BW2 and mBW2 surfaces. This is the important character of BW surfaces.
- (3) At high total energies ( $E_{\text{tot}} > 0.75 \text{ eV}$ ), the cross section increases with increasing  $j$  at a given total energy, and the rotational energy is more effective than translation energy.
- (4) The QCT results on the mBW2 PES are a little smaller than those of the experiment. However, they are a little larger than the rate constants modified by using eq 11 on BW2 surface. From this point, the mBW2 surface is better than the BW2 surface.

**Acknowledgment.** This work was supported by National Natural Science Foundation of China.

## References and Notes

- (1) Thompson, D. L.; Suzukava, H. H., Jr.; Raff, L. M. *J. Chem. Phys.* **1975**, *62*, 4727.
- (2) Weston, R. E., Jr. *J. Phys. Chem.* **1979**, *83*, 61.
- (3) Miller, J. C.; Gordon, R. T. *J. Chem. Phys.* **1983**, *78*, 3713.
- (4) Tucker, S. C.; Truhlar, D. G.; Garrett, B. C.; Isaacson, A. D. *J. Chem. Phys.* **1985**, *82*, 4102.
- (5) Schwenke, D. W.; Tucker, S. C.; Steckler, R.; Brown, F. B.; Lynch, G. C.; Truhlar, D. G.; Garrett, B. C. *J. Chem. Phys.* **1989**, *90*, 3110.
- (6) Ju, G.; Bian, W.; Davison, E. R. *Theor. Chim. Acta* **1992**, *83*, 331.
- (7) Bian W.; Ju, G. *Chem. J. Chin. Univ.* **1993**, *14*, 857.
- (8) Alagia, M.; Balucani, N.; Casavecchia, P.; Stranges, D.; Volpi, G. *J. Chem. Soc., Faraday Trans.* **1995**, *91*, 575.
- (9) Alagia, M.; Balucani, N.; Cartechini, L.; Casavecchia, P.; Van Kleef, E. H.; Vopli, G. G.; Aoz, F. J.; Bañares, L.; Schwenke, D. W.; Allison, T.; Mielke, S. L.; Truhlar, D. G. *Science* **1996**, *273*, 1519.

- (10) Allison, T. C.; Lynch, G. C.; Truhlar, D. G.; Gordon, M. S. *J. Phys. Chem.* **1996**, *100*, 13575.
- (11) Lee, S.-H.; Lai, L. H.; Liu, K. *J. Chem. Phys.* **1999**, *110*, 8229.
- (12) Skouteris, D.; Manolopoulos, D. E.; Bian, W.; Werner, H.-J.; Lai, L. H.; Liu, K. *Science* **1999**, *286*, 1713.
- (13) Aoiz, F. J.; Bañares, L.; Herrero, V. J. In *Advances in Classical Trajectory Methods Vol. III: Comparison of Classical and Quantum Dynamics*; Hase, W. L.; JAI: Greenwich, CT, 1998.
- (14) Aoiz, F. J.; Bañares, L.; Herrero, V. J. *J. Chem. Soc., Faraday Trans.* **1998**, *94*, 2483.
- (15) Kumaran, S. S.; Lim, K. P.; Michael, J. V. *J. Chem. Phys.* **1994**, *101*, 9487.
- (16) Stern, M. J.; Persky, A.; Klein, F. S. *J. Chem. Phys.* **1973**, *58*, 5697.
- (17) Persky, A. *J. Chem. Phys.* **1977**, *66*, 2932.
- (18) Persky, A. *J. Chem. Phys.* **1978**, *68*, 2411.
- (19) Persky, A. *J. Chem. Phys.* **1979**, *70*, 3910.
- (20) Persky, A.; Broida, M. *J. Chem. Phys.* **1986**, *84*, 2653.
- (21) Aoiz, F. J.; Bañares, L. *J. Phys. Chem.* **1996**, *100*, 18108.
- (22) Bian, W.; Werner, H.-J. *J. Chem. Phys.* **2000**, *112*, 220.
- (23) Manthe, U.; Bian, W.; Werner, H.-J. *Chem. Phys. Lett.* **1999**, *313*, 647.
- (24) Yang, B.; Gao, H.; Han, K.; Zhang, J. Z. H. *J. Chem. Phys.* **2000**, *113*, 1434.
- (25) Yang, B.; Tang, B.; Yin, H.; Han, K.; Zhang, J. Z. H. *J. Chem. Phys.* **2000**, *113*, 7182.
- (26) <http://thechem.edu.chinaren.com>
- (27) Werner, H.-J.; Knowles, P. J. *J. Chem. Phys.* **1988**, *89*, 5803.
- (28) Werner, H.-J.; Knowles, P. J. *J. Chem. Phys.* **1985**, *82*, 5053.
- (29) Langhoff, S. R.; Davidson, E. R. *Int. J. Quantum Chem.* **1974**, *8*, 61.
- (30) Steckler, R.; Schwenke, D. W.; Brown, F. B.; Truhlar, D. G. *Chem. Phys. Lett.* **1985**, *121*, 475.
- (31) Karplus, M.; Porter, R. N.; Sharma, R. D. *J. Chem. Phys.* **1965**, *43*, 3259.
- (32) Ju, G.; Feng, D.; Deng, C. *Theor. Chim. Acta* **1988**, *74*, 403.
- (33) Ju, G.; Feng, D.; Deng, C. *Sci Sinica, B* **1987**, *9*, 920.
- (34) Feng, K.; Wu, H.; Qin, M.; Wang, D. *J. Comput. Math.* **1989**, *7*, 71.
- (35) Yoshida, H. *Phys. Lett. A* **1990**, *150*, 262.
- (36) Schlier, Ch.; Seiter, A. *J. Phys. Chem. A* **1998**, *102*, 9939.
- (37) Aoiz, F. J.; Bañares, L.; Herrero, V. J.; Rábanos, V. S.; Stark, K.; Werner, H.-J. *Chem. Phys. Lett.* **1994**, *223*, 215.
- (38) Aoiz, F. J.; Bañares, L.; Herrero, V. J.; Rábanos, V. S.; Stark, K.; Werner, H.-J. *J. Phys. Chem.* **1994**, *98*, 10665.
- (39) Stark, K.; Werner, H.-J. *J. Chem. Phys.* **1996**, *104*, 6515.
- (40) Tully, J. C. *J. Chem. Phys.* **1974**, *60*, 3042.
- (41) Kita, D.; Stedman, D. H. *J. Chem. Soc., Faraday Trans.* **1982**, *78*, 1249.